HHS Public Access

Author manuscript

Cancer Genet. Author manuscript; available in PMC 2016 May 27.

Published in final edited form as:

Cancer Genet. 2015 June ; 208(6): 345–350. doi:10.1016/j.cancergen.2015.03.005.

ARID1A and *TERT* promoter mutations in dedifferentiated meningioma

Malak S. Abedalthagafi[1,*], **Wenya Linda Bi**[2,*], **Parker H. Merrill**[1], **William J. Gibson**[3], **Matthew F. Rose**[1], **Ziming Du**[1], **Joshua M. Francis**[4,5], **Rose Du**[2], **Ian F. Dunn**[2], **Azra H. Ligon**[6], **Rameen Beroukhim**[3,4,5], and **Sandro Santagata**[1,3,#]

[1]Department of Pathology, Division of Neuropathology, Brigham and Women's Hospital, Harvard Medical School, Boston, MA, USA

[2]Department of Neurosurgery, Brigham and Women's Hospital, Harvard Medical School, Boston, MA, USA

[3]Department of Cancer Biology, Dana-Farber Cancer Institute, Boston, MA, USA

[4]Department of Medical Oncology, Dana-Farber Cancer Institute, Boston, MA, USA

[5]Broad Institute of MIT and Harvard, Cambridge, MA, USA

[6]Clinical Cytogenetics Laboratory, Center for Advanced Molecular Diagnostics, Department of Pathology, Brigham and Women's Hospital, Harvard Medical School, Boston, MA, USA

Abstract

While WHO grade I meningiomas are considered benign, patients with WHO grade III meningiomas have very high mortality. The principles underlying tumor progression in meningioma are largely unknown yet a detailed understanding of these mechanisms will be required for effective management of patients with these high-grade, lethal tumors. We present a case of an intraventricular meningioma that at first presentation displayed remarkable morphologic heterogeneity – comprised of distinct regions independently fulfilling histopathologic criteria for WHO grade I, II and III designations. The lowest-grade regions had classic meningothelial features while the highest grade regions were markedly dedifferentiated. While progression in meningiomas is generally observed during recurrence following radiation and systemic medical therapies the current case offers us a snapshot into histologic progression and intratumor heterogeneity in a native, pre-treatment context. Using whole exome sequencing (WES) and high resolution array comparative genomic hybridization (aCGH) we observe marked genetic heterogeneity between the various areas. Notably, in the higher grade regions we find increased aneuploidy with progressive loss of heterozygosity, the emergence of mutations in the *TERT* promoter and compromise of *ARID1A*. These findings provide new insights into intratumoral heterogeneity in the evolution of malignant phenotypes in anaplastic meningiomas and potential pathways of malignant progression.

[#]Correspondence should be addressed to: Sandro Santagata, M.D., Ph.D., Assistant Professor of Pathology, Department of Pathology, Brigham and Women's Hospital, Harvard Medical School, Department of Cancer Biology, Dana-Farber Cancer Institute, 77 Avenue Louis Pasteur, Boston, MA 02115, Ph: 617-525-5686, Fax: 617-975-0944, ; Email: ssantagata@partners.org

[*]These authors contributed equally to this work

Conflict of interest: The authors declare no conflicts of interest with respect to this study.

Keywords

meningioma; anaplastic; progression; intratumoral heterogeneity; swi/snf complex; chromatin remodeling

Introduction

Meningiomas are the most common primary tumors of the central nervous system, with 10–15% following an aggressive course with rapid growth, invasion into adjacent structures, and rapid recurrence even after radical resection and adjuvant treatment. These meningiomas are classified as World Health Organization (WHO) grade II or III and are associated with premature mortality [1]. Despite emerging understanding of the genetic changes underlying meningioma formation [2–10], the factors that drive malignant progression in meningioma remain poorly understood [11–13]. We encountered a case of a unique untreated intraventricular meningioma, which allowed us to investigate molecular factors associated with tumor progression and dedifferentiation.

Materials and Methods

Pathologic examination

Histopathologic diagnosis and tumor purity >80% was confirmed by review of the H&E stained sections by two neuropathologists (S.S., M.A.). This study was approved by the human subject institutional review board of the Dana-Farber/Brigham and Women's Cancer Center.

Immunohistochemistry and RNAscope

Immunohistochemistry was performed using commercially available antibodies following standard automated and manual protocols on paraffin-embedded formalin-fixed tissue. The slides were incubated with antibodies for MIB-1 (Ki-67, Dako, Cat# M7240), epithelial membrane antigen (EMA, Dako, Cat# M0613 clone: E29) and ARID1A (monoclonal ARID1A/BAF250a, Cat# sc-32761X, Santa Cruz) and developed using 3,3′-diaminobenzidine (DAB) as the chromagen (Sigma Chemical Co., St. Louis, MO), before counterstaining with hematoxylin. Appropriate positive and negative controls were used throughout. In situ hybridization of *TERT* mRNA transcripts was performed using the RNAscope® assay with Probe-Hs-TERT (Cat# 605511, Advanced Cell Diagnostics, USA), following manufacturer's protocols [10,14].

Genomic analysis

Array-based comparative genomic hybridization (aCGH) was performed using a stock 1×1M Agilent SurePrint G3 Human CGH Microarray chip in a CLIA-certified laboratory. A minimum of 1.3μg DNA, corresponding to approximately 6×1mm FFPE punches, was obtained for each specimen. Genomic DNA isolated from FFPE blocks was hybridized with a commercial reference DNA sample representing a pool of individuals with normal karyotypes (Promega, Madison, WI). The array platform contains 963,029 probes spaced with a 2.1kb overall median probe spacing and a 1.8kb probe spacing in RefSeq genes

across the human genome. A genomic imbalance is reported when a minimum of eight consecutive probes, corresponding to approximately 14–16kb, show an average log2 ratio above +0.25 or below −0.5.

Whole-exome sequencing was performed on DNA isolated from each histopathologically distinct area, and matched germline DNA, to a mean depth of 80X, and analysis proceeded as previously described [8,15]. Raw sequencing data was processed using the Picard tools pipeline and the Genome Analysis Toolkit (GATK) [16,17]. Mutation analysis for single nucleotide variants (SNV) was performed using MuTect v1.1.4 [18], indel calling was performed using the GATK SomaticIndelDetector tool; SNVs and indels were annotated using Oncotator. To analyze somatic copy number alterations from whole exome data, we used the ReCapSeg algorithm, which assesses homologue-specific copy ratios (HSCRs) from segmental estimates of multipoint allelic copy-ratios at heterozygous loci incorporating the statistical phasing software (BEAGLE) and population haplotype panels (HAPMAP3) [19–21].

Results

A 48-year-old woman presented with five days of headache and gait instability, prompting imaging that revealed a 6.9×4.7×5cm heterogeneously contrast-enhancing mass, centered within the atrium of the right lateral ventricle, causing obstructive hydrocephalus (Fig. 1A–B). A right parietal craniotomy was performed with gross total resection of the tumor (Fig. 1C). The patient's symptoms improved post-operatively and she remains alive two years following the resection.

The histopathology was notable for the concurrent presence of regions displaying classic features of low-grade meningothelial meningioma (WHO grade I), others with features of atypical WHO grade II meningioma, and areas harboring cells with a pronounced increase in nucleocytoplasmic ratio, frequent mitosis and loss of discernable features of meningothelial differentiation – hallmarks of dedifferentiation in a WHO grade III anaplastic meningioma (Fig. 1D). Consistent with this histologic progression, the MIB-1 proliferation index ranged from <1% to >90% in corresponding grade I versus grade III regions (Fig. 1D). Immunohistochemistry (IHC) for epithelial membrane antigen (EMA), a marker of meningothelial differentiation, also showed EMA expression in the low-grade regions that was entirely lost in the highest-grade regions, consistent with the morphologic dedifferentiation (Fig. 1D). To better understand the molecular underpinnings of the histologic heterogeneity within this tumor, we analyzed DNA extracted from core punches from each of these three regions using high-resolution array-based comparative genomic hybridization (aCGH), Sanger sequencing of the *TERT* promoter, and whole-exome sequencing (Fig. 2).

The aCGH data showed partial single-copy loss of chromosomes 1p, 3q, 6q, 7p, 11q, 18q (monosomy 18), and 22q (monosomy 22) in all three areas (Fig. 2A). The atypical and anaplastic regions both harbored an expanded loss of chromosome 11q, additional unique losses of 4, 11p, and regions of 5, 15q, and 17q that were not detected in the grade I areas. Expansion of 5p and 9q losses was distinct to the grade III area, as were gains on

chromosome 8 and 10q. Copy-number analysis of the whole-exome sequencing data showed a similar pattern of losses and further revealed progressive loss of heterozygosity across the three regions and evidence for subclonal chromosomal losses in Area 2 that become clonal in Area 3 (Fig. 2B).

Because whole-exome sequencing does not cover the promoter region of the *TERT* gene, which has been reported to be mutated in meningiomas with histologic progression [2], we performed Sanger sequencing of this region. We found wild-type sequences in the grade I area but the C228T mutation in both the grade II and III areas. Using RNAscope *in situ* hybridization [14], we found that *TERT* mRNA is low in grade I areas and sharply increased in higher-grade areas (Fig. 2C). The whole-exome sequencing data revealed a low frequency of other mutations in the three samples with the notable presence of an *ARID1A* frameshift deletion (p.LHH2017fs) in the grade II and III areas (Supplementary Table 1). Coupled with single-copy loss of chromosome 1p, the frameshift would lead to a sharp decrease in ARID1A protein levels. Indeed, ARID1A levels are markedly reduced in the high-grade areas on IHC (Fig. 2D).

Discussion

The mutation and copy-number data reveal a concentric, rather than partially overlapping, pattern of alterations; nearly all mutations and copy number alterations in the areas with atypical histopathology were also observed in the sample with higher-grade anaplastic features. This suggests a common clonal origin to the distinct areas. Notably, this tumor was newly diagnosed, without prior surgical or chemo-radiation treatment. It is interesting to speculate that the *de novo* molecular heterogeneity observed in our case reflects a set of clonal sweeps where each ensuing clone consists of a subclone of the previous dominant clone (Fig. 2E). One might imagine that therapeutic interventions such as chemotherapy and radiation may precipitate a different pattern in which multiple surviving subclones compete for dominance.

The shared pattern of single-copy loss, involving chromosomes 1p, 3q, 6q, 18q, and 22q, is consistent with previously reported cytogenetic changes in high-grade meningiomas [22]. We found these alterations even in the areas with grade I histologic features, which had a low proliferative index and intact EMA expression, suggesting that additional alterations can be needed for histologic progression. Non-contiguous losses on 15q and 17q and the unique whole-arm loss of 9q observed only in the anaplastic region contrasts with previously observed gains of 9q, 15q, and 17q in some high-grade meningiomas and reflects the current incomplete understanding of the specific oncogenic drivers within these broad regions [13,22]. No *CDKN2A* (9p21.3) deletions, a frequent finding amongst aggressive meningiomas [13,23], were observed.

The differences in mutational profiles between the low (grade I) and high-grade (grades II and III) areas are intriguing. Mutations in the *TERT* promoter and in *ARID1A* were most notable. Telomerase activation is well-recognized as a feature of malignant meningiomas [24], with a recent report that *TERT* promoter mutations are specific to meningiomas which recur displaying histologic progression [2]. The observation of differential TERT expression

within regions of the same tumor that had not been treated further supports the role for increased TERT in the malignant progression of meningioma. Moreover, sequencing studies have revealed that the genes encoding subunits of mammalian SWI/SNF complexes are mutated in over 20% of all human cancers [25–27]. *ARID1A* is important in ensuring correct lineage progression and in limiting self-renewal [28]. It is interesting to propose that concomitant activation of TERT and compromise of the SWI/SNF complex or other chromatin remodeling complexes through a range of genetic or epigenetic events [29] may synergize in allowing meningioma cells to develop high-grade malignant phenotypes [12] and dedifferentiate.

Supplementary Material

Refer to Web version on PubMed Central for supplementary material.

Acknowledgments

We are grateful to Marian Slaney and Sebastian Valentino for assistance with histology, Terri Woo for assistance with immunohistochemistry and Marc L. Listewnik for cytogenetic data support for technical assistance. The work is supported by 35-1041 grant from King Abdulaziz City for Science and Technology (KACST), Saudi Arabia (M.A.A.), the Brain Science Foundation (S.S.) and the Jared Branfman Sunflowers for Life Fund for Pediatric Brain and Spinal Cancer Research (S.S.).

References

1. Wiemels J, Wrensch M, Claus EB. Epidemiology and etiology of meningioma. J Neurooncol. 2010; 99:307–314. DOI: 10.1007/s11060-010-0386-3 [PubMed: 20821343]
2. Goutagny S, Nault JC, Mallet M, Henin D, Rossi JZ, Kalamarides M. High Incidence of Activating TERT Promoter Mutations in Meningiomas Undergoing Malignant Progression. Brain Pathol. 2014; 24:184–189. DOI: 10.1111/bpa.12110 [PubMed: 24261697]
3. Abedalthagafi MS, Merrill PH, Bi WL, et al. Angiomatous meningiomas have a distinct genetic profile with multiple chromosomal polysomies including polysomy of chromosome 5. Oncotarget. 2014; 5:10596–10606. [PubMed: 25347344]
4. Smith MJ, O'Sullivan J, Bhaskar SS, et al. Loss-of-function mutations in SMARCE1 cause an inherited disorder of multiple spinal meningiomas. Nature genetics. 2013; 45:295–298. DOI: 10.1038/ng.2552 [PubMed: 23377182]
5. Sahm F, Bissel J, Koelsche C, et al. AKT1E17K mutations cluster with meningothelial and transitional meningiomas and can be detected by SFRP1 immunohistochemistry. Acta neuropathologica. 2013; 126:757–762. DOI: 10.1007/s00401-013-1187-5 [PubMed: 24096618]
6. Reuss DE, Piro RM, Jones DT, et al. Secretory meningiomas are defined by combined KLF4 K409Q and TRAF7 mutations. Acta neuropathologica. 2013; 125:351–358. DOI: 10.1007/s00401-013-1093-x [PubMed: 23404370]
7. Clark VE, Erson-Omay EZ, Serin A, et al. Genomic analysis of non-NF2 meningiomas reveals mutations in TRAF7, KLF4, AKT1, and SMO. Science. 2013; 339:1077–1080. DOI: 10.1126/science.1233009 [PubMed: 23348505]
8. Brastianos PK, Horowitz PM, Santagata S, et al. Genomic sequencing of meningiomas identifies oncogenic SMO and AKT1 mutations. Nature genetics. 2013; 45:285–289. DOI: 10.1038/ng.2526 [PubMed: 23334667]
9. Aavikko M, Li SP, Saarinen S, et al. Loss of SUFU function in familial multiple meningioma. American journal of human genetics. 2012; 91:520–526. DOI: 10.1016/j.ajhg.2012.07.015 [PubMed: 22958902]
10. Du Z, Abedalthagafi M, Aizer AA, et al. Increased expression of the immune modulatory molecule PD-L1 (CD274) in anaplastic meningioma. Oncotarget. 2014

11. Yang HW, Kim TM, Song SS, et al. Alternative splicing of CHEK2 and codeletion with NF2 promote chromosomal instability in meningioma. Neoplasia. 2012; 14:20–28. [PubMed: 22355270]
12. Kliese N, Gobrecht P, Pachow D, et al. miRNA-145 is downregulated in atypical and anaplastic meningiomas and negatively regulates motility and proliferation of meningioma cells. Oncogene. 2013; 32:4712–4720. DOI: 10.1038/onc.2012.468 [PubMed: 23108408]
13. Choy W, Kim W, Nagasawa D, et al. The molecular genetics and tumor pathogenesis of meningiomas and the future directions of meningioma treatments. Neurosurgical focus. 2011; 30:E6.doi: 10.3171/2011.2.FOCUS1116 [PubMed: 21529177]
14. Wang F, Flanagan J, Su N, et al. RNAscope: a novel in situ RNA analysis platform for formalin-fixed, paraffin-embedded tissues. J Mol Diagn. 2012; 14:22–29. DOI: 10.1016/j.jmoldx.2011.08.002 [PubMed: 22166544]
15. Brastianos PK, Taylor-Weiner A, Manley PE, et al. Exome sequencing identifies BRAF mutations in papillary craniopharyngiomas. Nature genetics. 2014; 46:161–165. DOI: 10.1038/ng.2868 [PubMed: 24413733]
16. DePristo MA, Banks E, Poplin R, et al. A framework for variation discovery and genotyping using next-generation DNA sequencing data. Nature genetics. 2011; 43:491–498. DOI: 10.1038/ng.806 [PubMed: 21478889]
17. McKenna A, Hanna M, Banks E, et al. The Genome Analysis Toolkit: a MapReduce framework for analyzing next-generation DNA sequencing data. Genome research. 2010; 20:1297–1303. DOI: 10.1101/gr.107524.110 [PubMed: 20644199]
18. Cibulskis K, Lawrence MS, Carter SL, et al. Sensitive detection of somatic point mutations in impure and heterogeneous cancer samples. Nature biotechnology. 2013; 31:213–219. DOI: 10.1038/nbt.2514
19. Altshuler DM, Gibbs RA, et al. International HapMap C. Integrating common and rare genetic variation in diverse human populations. Nature. 2010; 467:52–58. DOI: 10.1038/nature09298 [PubMed: 20811451]
20. Browning BL, Yu Z. Simultaneous genotype calling and haplotype phasing improves genotype accuracy and reduces false-positive associations for genome-wide association studies. American journal of human genetics. 2009; 85:847–861. DOI: 10.1016/j.ajhg.2009.11.004 [PubMed: 19931040]
21. Carter SL, Cibulskis K, Helman E, et al. Absolute quantification of somatic DNA alterations in human cancer. Nature biotechnology. 2012; 30:413–421. DOI: 10.1038/nbt.2203
22. Riemenschneider MJ, Perry A, Reifenberger G. Histological classification and molecular genetics of meningiomas. Lancet neurology. 2006; 5:1045–1054. DOI: 10.1016/S1474-4422(06)70625-1 [PubMed: 17110285]
23. Bostrom J, Meyer-Puttlitz B, Wolter M, et al. Alterations of the tumor suppressor genes CDKN2A (p16(INK4a)), p14(ARF), CDKN2B (p15(INK4b)), and CDKN2C (p18(INK4c)) in atypical and anaplastic meningiomas. The American journal of pathology. 2001; 159:661–669. DOI: 10.1016/S0002-9440(10)61737-3 [PubMed: 11485924]
24. Simon M, Park TW, Leuenroth S, Hans VH, Loning T, Schramm J. Telomerase activity and expression of the telomerase catalytic subunit, hTERT, in meningioma progression. Journal of neurosurgery. 2000; 92:832–840. DOI: 10.3171/jns.2000.92.5.0832 [PubMed: 10794298]
25. Wu JN, Roberts CW. ARID1A mutations in cancer: another epigenetic tumor suppressor? Cancer discovery. 2013; 3:35–43. DOI: 10.1158/2159-8290.CD-12-0361 [PubMed: 23208470]
26. Guan B, Wang TL, Shih Ie M. ARID1A, a factor that promotes formation of SWI/SNF-mediated chromatin remodeling, is a tumor suppressor in gynecologic cancers. Cancer research. 2011; 71:6718–6727. DOI: 10.1158/0008-5472.CAN-11-1562 [PubMed: 21900401]
27. Dykhuizen EC, Hargreaves DC, Miller EL, et al. BAF complexes facilitate decatenation of DNA by topoisomerase IIalpha. Nature. 2013; 497:624–627. DOI: 10.1038/nature12146 [PubMed: 23698369]
28. Eroglu E, Burkard TR, Jiang Y, et al. SWI/SNF complex prevents lineage reversion and induces temporal patterning in neural stem cells. Cell. 2014; 156:1259–1273. DOI: 10.1016/j.cell.2014.01.053 [PubMed: 24630726]

29. Kadoch C, Hargreaves DC, Hodges C, et al. Proteomic and bioinformatic analysis of mammalian SWI/SNF complexes identifies extensive roles in human malignancy. Nature genetics. 2013; 45:592–601. DOI: 10.1038/ng.2628 [PubMed: 23644491]

30. Craig JM, Vena N, Ramkissoon S, et al. DNA fragmentation simulation method (FSM) and fragment size matching improve aCGH performance of FFPE tissues. PLoS One. 2012; 7:e38881.doi: 10.1371/journal.pone.0038881 [PubMed: 22719973]

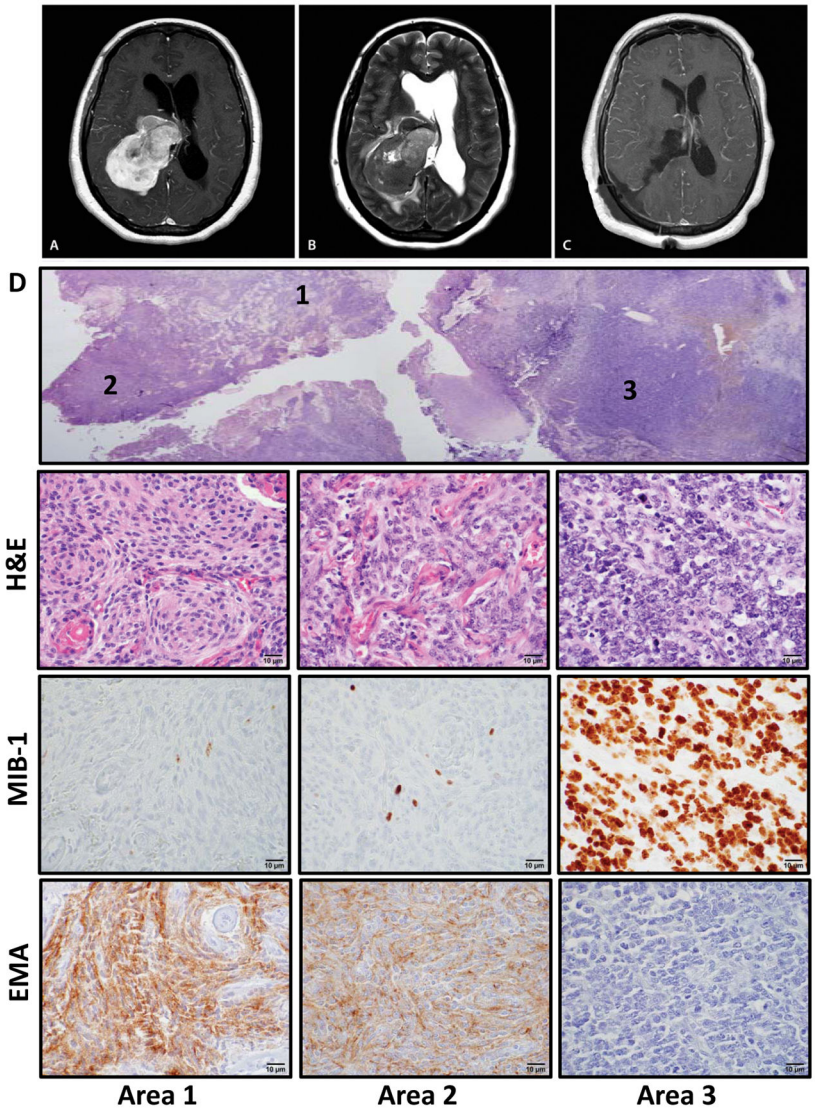

Figure 1.

Intratumoral heterogeneity within a high-grade meningioma. (A) T1-weighted gadolinium-enhanced axial MRI demonstrating a heterogeneously appearing contrast-avid tumor within the atrium of the right lateral ventricle, with (B) significant peritumoral edema and associated hydrocephalus on the T2-weighted axial MRI. (C) Post-operative T1-weighted axial MRI demonstrating complete resection. (D) Section of tumor, with 3 distinct appearing histologic regions (designated areas 1, 2, 3). Immunohistochemistry for epithelial membrane antigen (EMA) and MIB-1 (Ki-67). Scale bar, 10 μm.

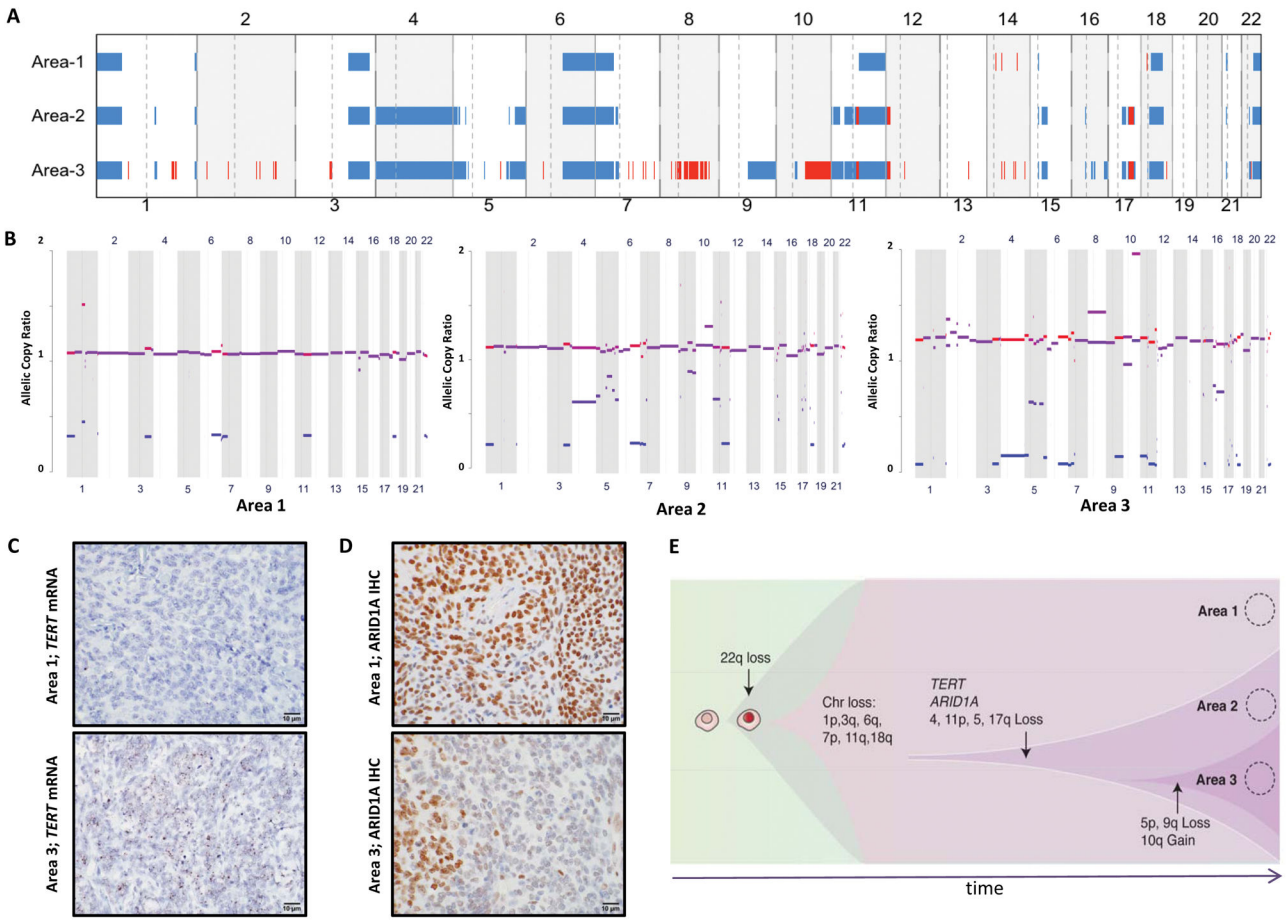

Figure 2.

Genetic heterogeneity within a high-grade meningioma. (A) High-resolution aCGH was performed on DNA extracted from core punches taken from area 1 (WHO grade I), area 2 (WHO grade II), and area 3 (WHO grade III), using 1×1M Agilent SurePrint G3 Human CGH Microarray chip [3,30]. Red indicates gain and blue indicates loss. (B) Copy number analysis from exome-sequencing data of the three areas shown as allelic copy ratios. Red indicates gain and blue indicates loss. (C) In situ hybridization of *TERT* mRNA transcripts using a *TERT*-specific RNAscope probe in FFPE sections of the meningioma samples [10,14]. (D) Immunohistochemistry for ARID1A. (E) Schematic representation of clonal evolution leading to dedifferentiation and intratumoral heterogeneity. Scale bar, 10 μm.